Nonlinear Saturation of Trapped Electron Modes via Perpendicular Particle Diffusion

F. Merz and F. Jenko

Max-Planck-Institut für Plasmaphysik, EURATOM Association, Boltzmannstrasse 2, 85748 Garching, Germany

(Received 8 August 2007; published 24 January 2008)

In magnetized fusion plasmas, trapped electron mode (TEM) turbulence constitutes, together with ion temperature gradient (ITG) turbulence, the dominant source of anomalous transport on ion scales. While ITG modes are known to saturate via nonlinear zonal flow generation, this mechanism is shown to be of little importance for TEM turbulence in the parameter regime explored here. Instead, a careful analysis of the statistical properties of the $\mathbf{E} \times \mathbf{B}$ nonlinearity in the context of gyrokinetic turbulence simulations reveals that perpendicular particle diffusion is the dominant saturation mechanism. These findings allow for the construction of a rather realistic quasilinear model of TEM induced transport.

DOI: 10.1103/PhysRevLett.100.035005 PACS numbers: 52.65.Tt, 52.30.Gz, 52.35.Ra

It is widely recognized that one of the key open issues in magnetic confinement fusion research is the analysis, prediction, and control of anomalous (i.e., turbulent) transport. However, despite significant progress in this area over the last several years, the theoretical understanding of the underlying physical phenomena—which are quite complex—is still far from being complete. This is even true for fundamental questions concerning, e.g., the nonlinear saturation mechanism of linear microinstabilities as will become clear in the present work. Such new insights are, of course, interesting in and of themselves, but at the same time, they are also of practical interest since they can be used to improve the accuracy of quasilinear transport models.

So far, most theoretical and computational research on anomalous transport in the core of fusion devices has focused on ion temperature gradient (ITG) turbulence in tokamaks, adopting the so-called adiabatic electron approximation (see, e.g., Ref. [1]). This development is, in part, due to the relatively good tractability of this problem. Consequently, the findings from such studies have become standard paradigms in our understanding of plasma microturbulence. A classic example for this is the role of zonal flows. As has been discussed extensively in the literature, adiabatic ITG turbulence generates $\mathbf{E} \times \mathbf{B}$ shear flows which are associated with purely radial fluctuations of the electrostatic potential; these zonal flows in turn regulate the turbulence via vortex shearing. This interplay constitutes the dominant saturation mechanism in these systems and therefore determines the level of anomalous transport (see, e.g., Refs. [2–5]).

It is clear, however, that ITG modes are not the only relevant source of core turbulence. In particular, many present-day (and future) fusion experiments rely on powerful electron heating systems which can turn trapped electron mode (TEM) turbulence into an important, if not dominant, agent of cross-field transport. In this Letter, we therefore investigate the saturation mechanism of fully developed, collisionless TEM turbulence driven by electron temperature gradients via computer simulations with the nonlinear gyrokinetic code GENE [6,7]. As it turns out, the results—which are, of course, helpful for a deeper understanding of anomalous transport in tokamak plasmas—can also be used to justify the quasilinear transport model employed in Refs. [7,8]. As has been shown in these papers, the latter may be used to reproduce several results from nonlinear computations which have been inaccessible in the past for such models.

All GENE simulations in this Letter are performed in $\hat{s}$-α geometry with $\alpha = 0$. The nominal plasma parameters, unless stated otherwise, are $R/L_{T_e} = 6$, $R/L_{T_i} = 0$, $R/L_n = 3$, $\beta_e = 10^{-3}$, $T_e/T_i = 3$, $m_e/m_i = 1/400$, $\hat{s} = 0.8$, $q = 1.4$, and $\epsilon \equiv r/R = 0.16$. This parameter set was motivated by experimental studies of plasmas with dominant electron heating [9] and has been used before in Ref. [7]. Note that we are considering pure, electron temperature gradient driven TEM turbulence here; electron temperature gradient modes are linearly stable due to the relatively cold ions [10], and there is no ITG drive. The perpendicular box size is given by $L_x = 165\rho_s$ and $L_y = 210\rho_s$, and the numerical resolution is $96 \times 128 \times 16 \times 32 \times 8$ points in the radial, binormal, parallel, $v_\parallel$, and μ directions, respectively. (For convergence studies concerning velocity space resolution, see Ref. [7].)

In a first step, we would like to assess the role of zonal flows in collisionless TEM turbulence. To this end, we compare ''normal'' TEM simulations to runs in which the zonal modes are artificially zeroed out. Time traces of the electron heat flux for one pair of simulations with and without zonal flows for the nominal parameters are shown in Fig. 1. Although one observes differences in the initial (transient) saturation phase, the transport level in the physically relevant quasistationary state remains the same, implying that zonal flows are not the dominant saturation mechanism. This behavior is very different from the well studied (adiabatic) ITG case, where the suppression of zonal flows typically leads to a significant increase of the heat flux (by an order of magnitude or more) [2–4].

In order to study the dependence of this result on the strength of the turbulence drive, we also performed other

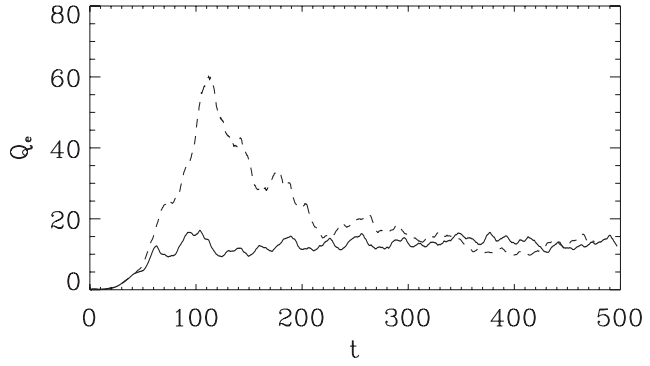

FIG. 1. Time evolution (in units of L_n/c_s) of the electron heat flux Q_e (in units of $\rho_s^2 c_s p_{e0}/L_n^2$) for a TEM simulation with (solid line) and without (dashed line) zonal flows.

pairs of simulations for different values of R/L_{T_e}. As R/L_{T_e} decreases from the nominal value to zero, the underlying TEM instability changes from an electron temperature gradient driven type to a purely density gradient driven one. As can be seen in Fig. 2, this linear property translates into the absence of a critical electron temperature gradient in the nonlinear runs, although the electron heat flux becomes comparatively small for $R/L_{T_e} \to 0$. More importantly in the present context, the artificial suppression of zonal flows leads to a significant relative increase of the electron heat flux if the turbulence is sustained by density gradient driven TEMs, in line with Ref. [11]. However, a very different behavior can be observed for reasonably large electron temperature gradients, characteristic of the majority of fusion plasmas. Although there might be different cases [12], for these plasma parameters, zonal flows have practically no impact on the saturated transport level, implying that the dominant saturation mechanism must be of a different nature. The questions of what this mechanism is and how we can describe it are the subject of the remainder of this Letter.

The present simulations are based on the gyrokinetic Vlasov-Maxwell system of equations which describes the self-consistent interaction of the gyro-averaged particle distribution functions with the corresponding electromagnetic fields [13]. It can be written symbolically as

$$\frac{\partial g}{\partial t} = \mathcal{L}g + \mathcal{N}[g], \tag{1}$$

where $g(s, x, y, z, v_\parallel, \mu, t)$ is the (modified) distribution function which depends on the species, radial, binormal, parallel (spatial), parallel velocity, and magnetic moment coordinates as well as on time. $\mathcal{L}$ is a linear integro-differential operator acting on g, and $\mathcal{N}[g]$ is a nonlinear integro-differential operator representing the (quadratic) $\mathbf{E} \times \mathbf{B}$ nonlinearity. For the exact form of $\mathcal{L}$ and $\mathcal{N}[g]$, see Ref. [7].

Interestingly, if one performs nonlinear TEM simulations, allowing the system to develop saturated turbulence, the resulting quasistationary state still exhibits many linear properties. For example, the amplitude spectrum of the electrostatic potential ϕ is, as the linear growth rate spectrum, centered around $k_x = 0$ (reflecting a dominance of radially elongated streamers); also, the phase relations between various pairs of fluctuating quantities [like (ϕ, n) or $(\phi, T_\perp)$] are very close to the values obtained in linear computations [7,8]. Moreover, as is shown in Fig. 3, the nonlinear values of the real frequency ω_r [calculated via $\mathrm{Im}[\ln(\phi_n/\phi_{n-1})]/\Delta t_{n-1/2}$ and averaged over time and the parallel coordinate, where n is a time step label and $k_x = 0$] match the respective linear results in the low k_y regime. It is only for $k_y \gtrsim 0.6$ that the results begin to differ. Here, the (time averaged) nonlinear frequency tends to zero for increasing k_y, whereas $|\omega_r|$ of the linear modes increases further (the negative sign indicates a drift in the electron diamagnetic direction). In order to explain these findings, we thus have to identify a nonlinear saturation mechanism which leaves various linear properties intact and is not related to zonal flow shearing.

In an attempt to quantify the statistical properties of the $\mathbf{E} \times \mathbf{B}$ nonlinearity which is responsible for saturating the linearly unstable modes, we choose to make the ansatz $\mathcal{N}[g] \propto g$. This implies that Eq. (1) can be rewritten as an

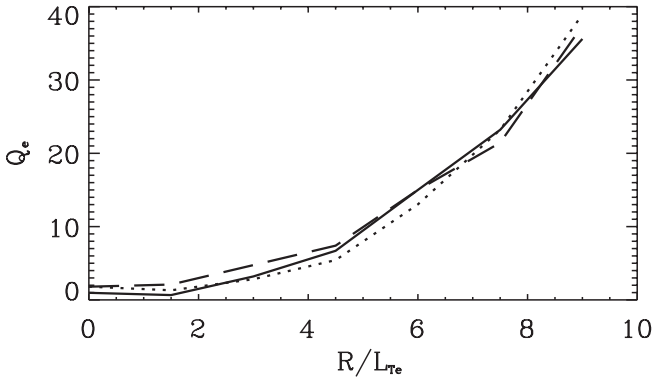

FIG. 2. Electron heat flux Q_e (in units of $\rho_s^2 c_s p_{e0}/L_n^2$) as a function of R/L_{T_e} for TEM simulations with (solid line) and without (dashed line) zonal flows. The dotted line depicts Q_e^{model} referred to later in the text.

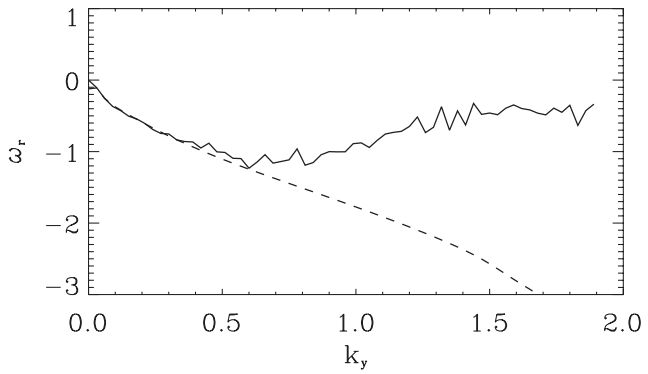

FIG. 3. Real frequency (in units of c_s/R) as a function of k_y (in units of $1/\rho_s$) for nonlinear (solid line) and linear (dashed line) TEM simulations.

effective linear equation,

$$\frac{\partial g}{\partial t} = \mathcal{L}g + \mathcal{X}g, \tag{2}$$

where we have introduced a model constant $\mathcal{X} \approx \mathcal{N}[g]/g$ with the dimension of a frequency. In the following, we explore the properties of $\mathcal{X}$ by means of nonlinear gyrokinetic simulations with GENE. The model assumption above is only a statistical relation; minimizing the squared error $\langle|\mathcal{N}[g] - \mathcal{X}g|^2\rangle$ yields $\mathcal{X} = \langle g^* \mathcal{N}[g]\rangle/\langle|g|^2\rangle$. To reduce the amount of data and obtain a manageable model, we consider $\mathcal{X}$ to depend only on the spatial coordinates and the species label; $\langle\,\rangle$ then denotes averaging over time and velocity space. To get a measure for the validity of Eq. (2), we calculate (in a second simulation) the normalized error of the real part, $\mathrm{err}_{\mathrm{Re}} = \langle|\mathrm{Re}(\mathcal{N}[g] - \mathcal{X}g)|^2\rangle^{1/2}/\langle|g|^2\rangle^{1/2}$, and its counterpart $\mathrm{err}_{\mathrm{Im}}$.

The k_y dependence of $\mathcal{X}$ for $k_x = 0$ and $z = 0$ (low-field side) is displayed in Fig. 4. Here, we chose to show the electron data, but the ion results are very similar. The solid line depicts the average value, while the bars indicate the model error as defined above. One can clearly distinguish two k_y ranges with rather different properties. For $|k_y| \gtrsim 0.3$, one finds a more or less constant (and small) real part of $\mathcal{X}$, an imaginary part which is roughly proportional to k_y, as well as large deviations from the model. For the much more important, transport dominating scales with $|k_y| \lesssim 0.3$, we find completely different properties, namely, a clearly discernible structure in the average values together with a very low fluctuation level. Because of its practical importance for heat and particle transport, we focus on this low k_y regime in the following.

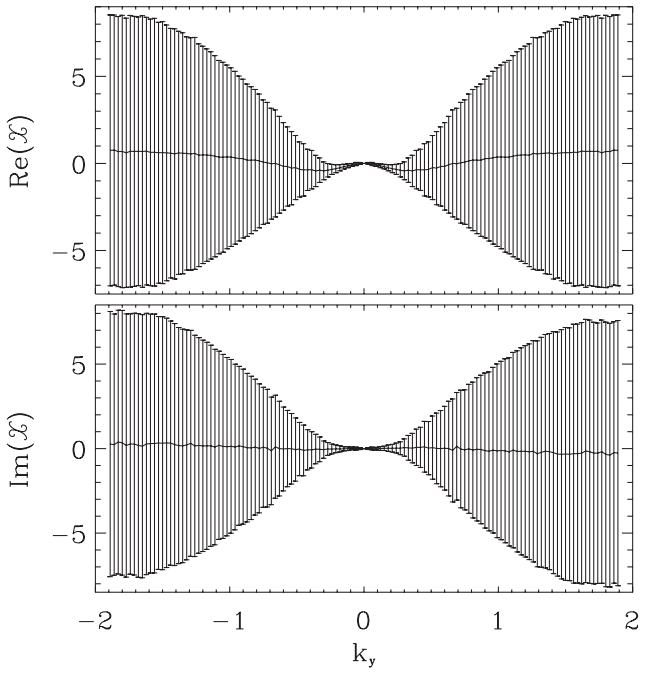

FIG. 4. Real and imaginary part of the quantity $\mathcal{X}$ in units of c_s/R. The bars indicate the model error as defined in the text.

The k_y dependence of $\mathcal{X}$ for $k_x = 0$, now averaged over the parallel direction z, is shown (for a smaller region around $k_y = 0$) in Fig. 5. One finds that the imaginary part of $\mathcal{X}$ is very close to zero for $|k_y| \lesssim 0.3$, meaning that g and $\mathcal{N}[g]$ are (almost) in phase. The corresponding real part, in contrast, is not zero, and its k_y dependence is well represented by a parabola through the origin. Combining these results for the real and imaginary parts, we can finally write

$$\mathcal{X} \approx -Dk_y^2, \tag{3}$$

implying that the overall effect of the $\mathbf{E} \times \mathbf{B}$ nonlinearity on the large, transport dominating scales is well described by perpendicular particle diffusion. This kind of behavior is in line with analytical results obtained, e.g., in the framework of Dupree's resonance broadening theory [14] and is qualitatively consistent with the nonlinear damping expected in the long-wavelength limit of other renormalized turbulence theories [15]. (Modern renormalized theories [15] also include nonlinear forcing terms which are related to the scatter represented by the bars in Fig. 4.) Moreover, it is consistent with the notion of dressed test modes in a bath of stochastic small-scale fluctuations [16]. However, to our knowledge, this is the first time that such phenomena have been observed directly in first-principles (gyrokinetic) simulations of plasma microturbulence, demonstrating their relevance for the nonlinear saturation of (electron temperature gradient driven) trapped electron modes.

It is worth pointing out that the result represented by Eq. (3) can nicely explain all the general observations about the similarity of nonlinear and linear runs mentioned above. First, an additional perpendicular diffusion term does not affect the eigenmodes of the linear operator $\mathcal{L}$ in Eq. (2); since $\mathcal{L}$ is block diagonal in k_y, the diffusivity induces only a spectral shift of the eigenvalues. This means that although the effective growth rate of the quasilinear

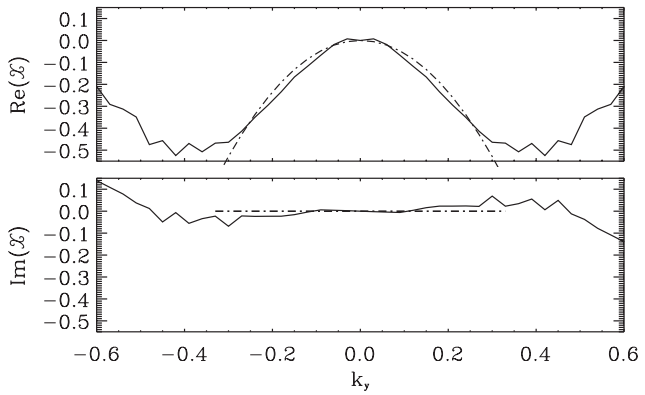

FIG. 5. The quantity $\mathcal{X}$ in units of c_s/R in the transport dominating region. The real part can be fitted by a parabola, the imaginary part by a constant (zero).

equation can approach zero (we find that the nonlinear damping rate is comparable to the linear growth rate for low k_y), the cross phases remain at the linear values, as observed in the simulations.

For higher values of k_y, where the diffusion approximation breaks down, the positive value of $\mathrm{Re}(\mathcal{X})$ in Fig. 4 corresponds to a nonlinear destablilization. This could be balanced by linear Landau damping, but as can be seen from the error bars, effects that are neglected in our approximation (like a nonlinear forcing term) do play an important role in this range. The same applies for the real frequency: The mean value of the nonlinear frequency shift $\mathrm{Im}(\mathcal{X})$ at larger values of k_y helps explain the results in Fig. 3, but obviously the frequency spectrum of the nonlinear forcing dominates.

Another important result is related to the dotted curve in Fig. 2. It shows $Q_e^{\mathrm{model}} = c_0 D(R/L_{T_e} + R/L_n)$, where the diffusivity $D = D(R/L_{T_e})$ is determined from quadratic fits to the low k_y range of $\mathrm{Re}(\mathcal{X})$ in various nonlinear simulations, and c_0 is a scalar fit parameter ($c_0 = 0.3$ in this case). The plot clearly exhibits a good quantitative correlation between the heat transport calculated from the diffusivity D and the heat transport directly obtained from the simulations.

These findings can be used to justify a refined quasilinear transport model which has been described in Refs. [7,8,17] and used successfully to reproduce various nonlinear simulation results which are difficult, if not impossible, to capture in more conventional models of this type. To this aim, we now retain the parallel structure of the diffusivity D occurring in Eq. (3). As is shown in Fig. 6, the diffusion term, taking into account the parallel change of $k_\perp^2$ due to the metric coefficients, peaks on the low-field side and exhibits a ballooning mode structure which is typical for curvature driven microinstabilities like TEMs. It is thus reasonable to expect that a dressed eigenmode with wave number k_y saturates when $\gamma_{\mathrm{eff}} \equiv \gamma_l(k_y) - k_y^2 \|D(z)(1 + \hat{s}^2 z^2)\|$ [with $\|f(z)\| \equiv L_s^{-1} \int_{-L_s/2}^{L_s/2} f(z)dz$] approaches zero. Given the fact that, according to Fig. 6, the nonlinear $D(z)$ can be approximated reasonably well by the parallel structure of the linear (squared) electrostatic potential $|\phi_{k_y}|^2(z)$, one finally obtains the model

$$Q_e \propto \max_{k_y}\left[\frac{\gamma_l(k_y)}{k_y^2(1 + \hat{s}^2\|z^2\|)}\right]\left(\frac{R}{L_{T_e}} + \frac{R}{L_n}\right) \qquad (4)$$

for the full (advective and diffusive) electron heat flux Q_e, where $\|z^2\| \approx \int z^2 |\phi_{k_y}|^2(z)dz / \int |\phi_{k_y}|^2(z)dz$ which helps to avoid a divergence as $k_y \to 0$ [7,8]. The subdominant ion heat and particle fluxes, Q_i and Γ, are then computed from the quasilinear ratios for the k_y which maximizes the right-hand side expression in Eq. (4). This model is able to capture various key features of TEM turbulence as has been discussed in Refs. [7,8].

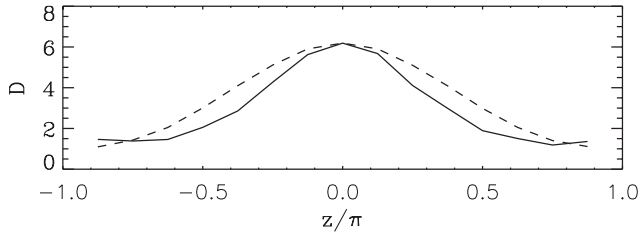

FIG. 6. Parallel structure of the diffusivity D (solid line) and of the linear squared amplitude $|\phi_{k_y}|^2$ (dashed line).

In summary, we have shown by a careful analysis of gyrokinetic turbulence simulations that in the parameter regime explored here, the nonlinear saturation mechanism for electron temperature gradient driven trapped electron modes is not zonal flow generation (in contrast to the ITG case), but perpendicular particle diffusion. Statistically, the action of the $\mathbf{E} \times \mathbf{B}$ nonlinearity on the long-wavelength, transport dominating modes can be expressed by a simple diffusion term, in line with the notion of dressed test modes in a bath of random small-scale fluctuations. This finding is not only able to explain the observed resemblance between linear and nonlinear modes, but can also serve to develop and justify new, improved kinds of quasilinear transport models which are in very good agreement with fully nonlinear simulations.

We would like to thank T. Görler, T. Dannert, and R. Friedrich for useful discussions. The computations were performed at the Garching Computer Center.

[1] A. M. Dimits *et al.*, Phys. Plasmas **7**, 969 (2000).
[2] G. W. Hammett *et al.*, Plasma Phys. Controlled Fusion **35**, 973 (1993).
[3] B. I. Cohen *et al.*, Phys. Fluids B **5**, 2967 (1993).
[4] A. M. Dimits *et al.*, Phys. Rev. Lett. **77**, 71 (1996).
[5] P. H. Diamond *et al.*, Plasma Phys. Controlled Fusion **47**, R35 (2005).
[6] F. Jenko *et al.*, Phys. Plasmas **7**, 1904 (2000).
[7] T. Dannert and F. Jenko, Phys. Plasmas **12**, 072309 (2005).
[8] F. Jenko, T. Dannert, and C. Angioni, Plasma Phys. Controlled Fusion **47**, B195 (2005).
[9] F. Ryter *et al.*, Phys. Rev. Lett. **95**, 085001 (2005).
[10] F. Jenko *et al.*, Phys. Plasmas **8**, 4096 (2001).
[11] D. R. Ernst *et al.*, Phys. Plasmas **11**, 2637 (2004).
[12] D. R. Mikkelsen (private communication).
[13] A. J. Brizard and T. S. Hahm, Rev. Mod. Phys. **79**, 421 (2007).
[14] T. H. Dupree, Phys. Fluids **10**, 1049 (1967).
[15] J. A. Krommes, Phys. Rep. **360**, 1 (2002).
[16] K. Itoh, S.-I. Itoh, and A. Fukuyama, *Transport and Structural Formation in Plasmas* (IOP Publishing, Bristol, U.K., 1999).
[17] M. Kotschenreuther *et al.*, Phys. Plasmas **2**, 2381 (1995).